Collisional Depolarization in Laser-Induced Fluorescence of OH†

Elizabeth A. Brinkman‡ and David R. Crosley*

Molecular Physics Laboratory, SRI International, Menlo Park, California 94025

Received: February 20, 2004

Laser-induced fluorescence in a flame can be polarized when excited by a polarized laser beam. This can produce apparently anomalous rotational line intensities resulting in errors in concentration and temperature measurements. Collisional depolarization does occur, but it must compete with vibrational and rotational energy transfer and quenching and is therefore not complete. We have measured collisional depolarization of LIF in OH at room temperature, using a discharge flow cell. The cross sections for $F_1(4)$ in the A state ($v' = 0$) are 3 Å^2 for the He collider, 15 Å^2 for nitrogen, 6 Å^2 for oxygen, 9 Å^2 for carbon dioxide, 20 Å^2 for argon, and an upper limit of 30 Å^2 for water. For He as a collider, the cross sections for $F_1(2)$ and $F_1(1)$ are 6 Å^2 and 9 Å^2, respectively.

Introduction

Excitation of molecules using polarized laser light produces polarized fluorescence emission. The interaction of the electric field vector of the laser with the transition dipole moments of the molecules preferentially excites those molecules whose transition dipoles are parallel with the laser electric vector. As a result, an aligned population is created. The molecules make many rotations prior to emitting a photon, but the alignment is not completely lost. This is because the total angular momentum J and its projection m_J on some laboratory axis are constants of the motion. Thus, the emitted fluorescence will be polarized. As a result, the accurate measurement of fluorescence intensities requires a consideration of polarization biases in the detection system.

The alignment of the transition dipole moment and the J vector depends on the rotational branch. In OH, the $A^2\Sigma^+ - X^2\Pi_i$ transition is a perpendicular transition: the transition dipole moment is perpendicular to the molecular axis. In general for Q branch transitions, the J vector and the transition dipole moment will be approximately parallel, i.e., the transition dipole is perpendicular to the plane of rotation, while for R and P branch transitions, the J vector and the transition dipole will be approximately perpendicular; i.e., the transition dipole will be in the plane of rotation. Thus, the polarization of the fluorescence will depend on the type of transition pumped and the type of transition observed in emission. The intensities expected under collision free conditions can be calculated from theory.[1,2]

The amount of polarization in the emission of a laser-induced fluorescence experiment depends on several factors in addition to the pumped and observed emission branches. The direction of detection relative to the laser electric vector will also affect the observed polarization, since an anisotropic population is generated by the laser. The amount of polarization is also affected by the degree of saturation of the pumped transition.[2] As a transition approaches saturation, less polarization will be observed. Last, collisions of the excited molecule with other gases will affect the amount of polarization observed. In addition to causing depolarization, collisions can cause vibrational energy transfer, rotational energy transfer, and quenching. All of these other processes remove molecules from the initially excited level, essentially freezing in the alignment of the m_J levels unless significant elastic depolarization occurs. Thus, the amount of polarization observed will depend on the relative rates of depolarization and the rates for these processes: if the depolarization rate is much greater than those for the other collisional processes, the emission will be depolarized, whereas if the depolarization rate is much less than those for the other collisional processes, the emission will be highly polarized.

Laser-induced fluoresence of OH is a useful tool in both flame diagnostics[3] and atmospheric monitoring.[4] We report here collisional depolarization of LIF of OH (A−X, $v' = 0$). in order to consider the effects of collisional depolarization on such monitoring, as well as an understanding of fundamental collision parameters. In fact, polarized fluorescence has been observed in a flame at atmospheric pressure,[1] and polarization spectoscopy (using two lasers) has been used to detect OH and measure the temperature.[5] The present experiments were performed at low pressures, where we could monitor the effects of individual colliders. In addition to their applications to diagnostics, these results will help us better understand the dynamics of collisions with small molecules. High quality ab initio calculations exist for the interaction of OH A state with He[6] and Ar[7] and quantum scattering calculations for rotational energy transfer cross sections are in excellent agreement with recent measurements. Because depolarization involves a change of m_J in a rotationally elastic collision, these measurements will provide a further test of these surfaces and the quantum scattering calculations.

Experimental Details

OH molecules were generated in a low-pressure flow cell by the reaction of hydrogen atoms and NO_2; hydrogen atoms were produced in a microwave discharge from a flow of hydrogen molecules in helium or argon. Operating pressures were typically 1−2 Torr.

The (0,0) band of the A−X system in OH was excited using the output of a frequency doubled, YAG pumped dye laser.

† Part of the special issue "Richard Bersohn Memorial Issue".

‡ Present address: Hitachi Global Storage Technologies, San Jose, California.

10.1021/jp040155j CCC: $27.50
Published on Web 08/06/2004

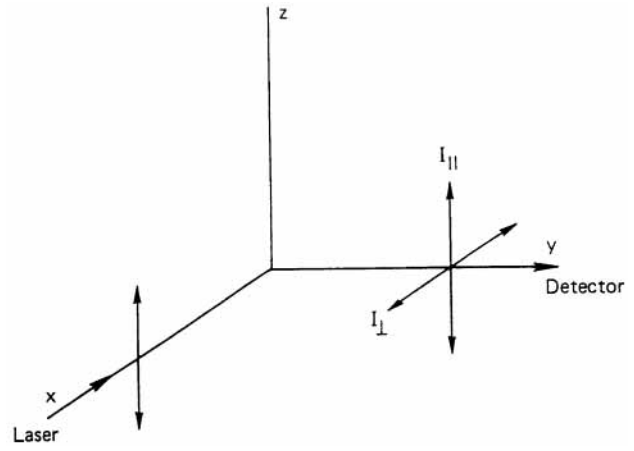

Figure 1. Coordinate system used to define the experimental configuration. The laser propagates along the *x* direction with its electric field vector polarized along the *z* axis. The fluorescence observation is in the *y* direction, observing light polarized parallel to the laser polarization (along *z*) or perpendicular to it (along *x*).

Typically 10 μJ pulse energy was used in an unfocused 350 μm diameter beam to avoid saturation. Experiments were performed using both linear and circularly polarized laser beams. The laser beam was >90% vertically polarized, measured using a sheet polarizer (Oriel) with an extinction ratio of 0.05. The beam was passed through the sheet polarizer prior to introduction into the cell and the cell windows were oriented at Brewster's angle to remove the other polarization components. For scans performed using circularly polarized light, a scrambler replaced the sheet polarizer just prior to the cell.

Fluorescence was viewed at right angles to the laser beam (Figure 1). The laser beam is incident along the *x*-axis, and polarized in the *z*-direction. The fluorescent light is collected in the *y*-direction, and may be polarized parallel or perpendicular to the laser polarization. As a measure of the polarization, we have used the ratio of the Q/P branch intensity in light polarized parallel to the laser polarization and also the ratio of the parallel to the perpendicular intensity in the Q branch.

Polarization of the fluorescence was analyzed using a sheet polarizer, rotated to transmit the fluorescence oriented parallel or perpendicular to the laser beam polarization. The fluorescence was then collimated and directed through a scrambler into a monochromator. The scrambler should remove any polarization-dependent spectral biases in the detection system. The monochromator (0.35 m focal length) was operated in second order, using 60 μm slits, which provided adequate resolution of the individual rotational lines. The photons were detected using a photomultiplier tube (1P28). A second photomultiplier tube, with only a UV transmitting filter, also located at right angles to the laser beam, collected the total fluorescence; this provided a normalization of the signal for fluctuations in laser power and OH concentration. The amplified output from both photomultiplier tubes was fed into gated integrator and boxcar averagers; the output from the monochromator PMT was also fed into a transient recorder with a signal averaging memory (Transiac Models 2001S and 4100). The entire experiment was controlled by a 486 computer, interfaced to the experiment via a CAMAC crate.

Results

Emission scans under nearly collision free conditions were performed by exciting the $Q_1(4)$ line in the (0,0) band of the A−X system of OH, using both circularly and linearly polarized light. This produces the $N' = 4$, $J' = 4.5$ rotational level in the $v' = 0$ level of the A state, termed the $F_1(4)$ level. Excitation with circularly polarized light allows a comparison of the "depolarized" emission spectrum with the linearly polarized emission spectrum. (Although circularly polarized light is not generally equivalent to unpolarized light, it does produced unpolarized emission in the geometry chosen.) A narrow detection gate of 7 ns, fwhm, is used, triggered promptly (about 15 ns) after the laser is fired; 10 shots are averaged per point. Figure 2A shows a fluorescence scan performed using circularly polarized light. The expected transitions, with no rotational energy transfer are $R_1(3)$, $Q_1(4)$, $Q_2'(4)$, $P_1(5)$, and $P_2'(5)$. The relative intensities of these peaks can be predicted from their line strengths. Fluorescence scans using vertically polarized laser light, detecting fluorescence polarized parallel to the laser polarization (Figure 2B) and perpendicular to the laser polarization (Figure 2C), show quite different relative peak intensities.

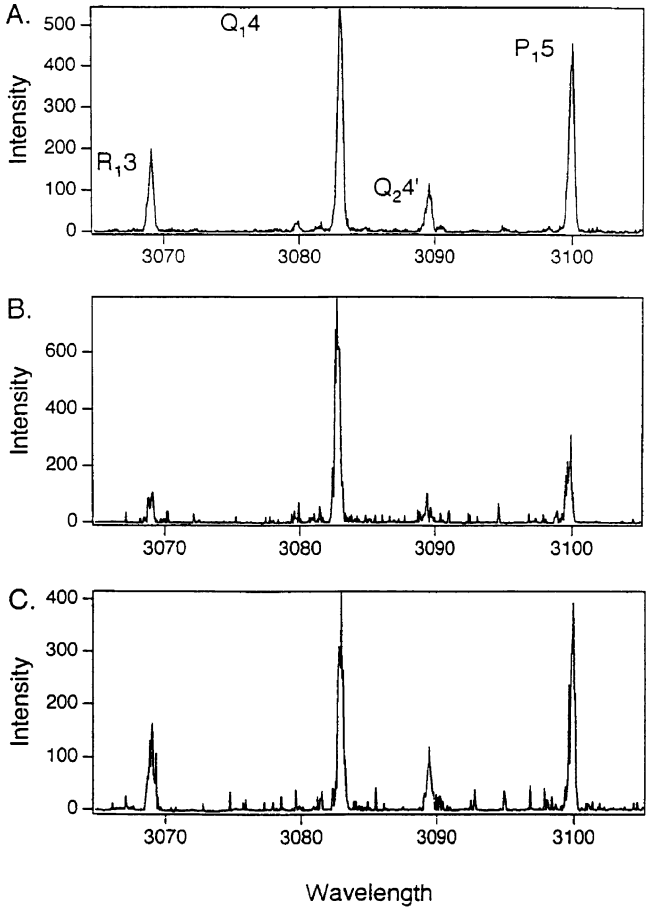

Figure 2. Fluorescence scans of the (0,0) band following excitation by the $Q_1$4 line, using a prompt trigger (approximately 15 ns) and a narrow gate (7 ns fwhm). Wavelength is given in Å. (A) Fluorescence observed using a scrambler prior to the cell, with no polarization analysis of the fluorescence. (B) Fluorescence observed using linearly polarized light, with the fluorescence observed in polarization parallel to the laser polarization. (C) Fluorescence observed using linearly polarized light, with the fluorescence observed in polarization perpendicular to the laser polarization.

Collisional depolarization was measured as a function of time and collider. The $F_1(4)$ level was excited via the $Q_1(4)$ transition. As a measure of depolarization, the ratio of the $Q_1(4)$ to $P_1(5)$ fluorescence was obtained in the parallel orientation. Depolarization can be studied by the ratio of the parallel to the perpendicular polarization intensity in either branch, or equivalently by this ratio of Q to P branch intensities in either

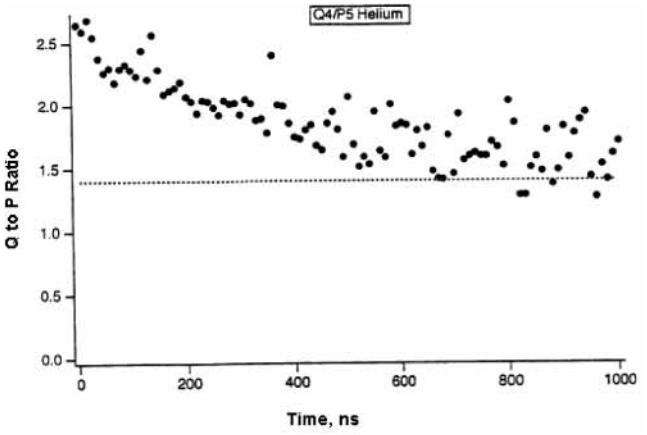

Figure 3. Intensity ratios $Q_1$4:$P_1$5 as a function of time in helium gas (1.6 Torr). The dashed line is the ratio of the line strengths.

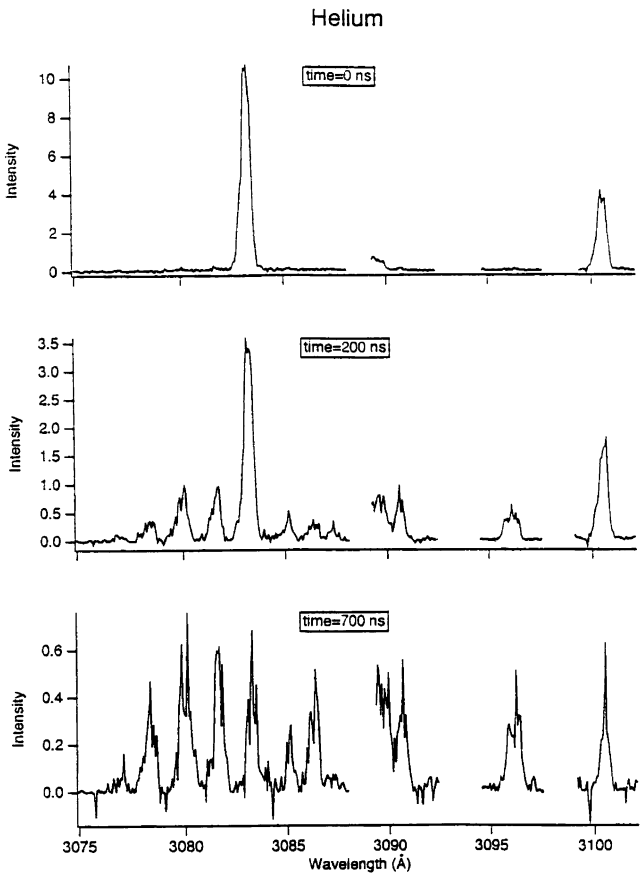

Figure 4. Fluorescence scans ((0,0 band) in helium at various delays after the laser is fired.Excitation by $Q_1(4)$. (A) Time = 0 ns. (B) Time = 200 ns. (C) Time = 700 ns. The R region (left) and P region (right) are shown.

polarization alone. The monochromator was scanned over these peaks; at each step 400 transients were collected and averaged. From these transients, spectra at 10 ns intervals were generated. The ratios of the areas of these peaks were plotted as a function of time to determine the depolarization rates. An example of data obtained in helium is shown in Figure 3.

Depolarization was also studied for other rotational levels which were populated by collisional energy transfer from $F_1(4)$. Spectra obtained in the parallel orientation in helium ($Q_1(4)$ pump) are shown for three time delays in Figure 4; extensive RET is seen at the long time delays.

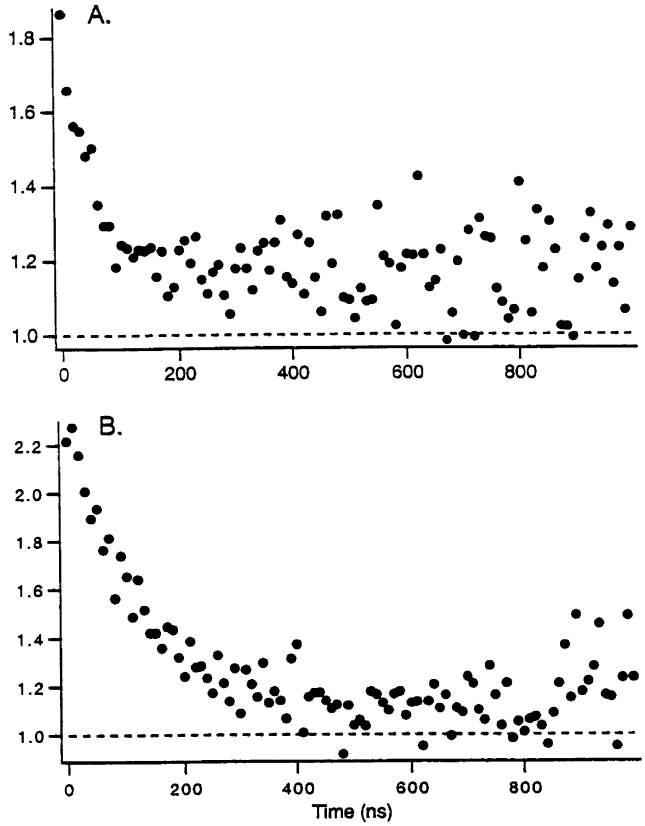

Figure 5. Intensity ratio for Q(parallel):Q(perpendicular) in helium: (A) $Q_1(1)$ pump; (B) $Q_1(2)$ pump.

Collisional depolarization was also measured in helium for $F_1(2)$ and $F_1(1)$ by exciting the $Q_1(2)$ and $Q_1(1)$ transitions, respectively. In these cases, to measure the depolarization, we obtained the ratio of the parallel to perpendicular fluorescence emission for each of these transitions, as a function of time. This is shown in Figure 5.

Collision-Free Polarization. The amount of polarization under collision-free conditions is determined by the angular momentum characteristics of the molecular state and transitions involved. In ref 1, a derivation is presented and the results are given, in tabular form, for the calculation of the degree of polarization. The fraction of the light polarized parallel and perpendicular to the laser polarization vector is given for all possible schemes: RR, RP, PP, QQ, RQ, and PQ, where the branches refer to pump and detection lines without respect to ordering.

From this we can calculate, for example, the ratio of intensities for the $Q_1(4)$ to $P_1(5)$ branch in emission, following excitation via $Q_1(4)$ in the absence of collisions. This ratio should be 3.5 for light polarized parallel to the laser polarization and 0.68 for light polarized perpendicular to it.

Results for the experimentally measured ratios are shown in Figure 2 for excitation of $Q_1(4)$. Under these conditions, the excited OH has lived an insufficient period of time to suffer collisions with the background He, even though it is present at a pressure of more than a Torr; very little rotational transfer is seen in these spectra. Dramatic differences are seen between the depolarized (Figure 2A), parallel polarized (Figure 2B) and perpendicularly polarized (Figure 2C) fluorescence spectra. The Q/P ratios are 1.3, 3.0, and 1.1, respectively.

We discovered, in accord with the expectations from ref 2, that saturation of the optical transition strongly affected the degree of polarization attainable. A measure of the degree of

TABLE 1

gas	depolarization cross section, Å^2	RET cross section, Å^2	RET ref
N_2	15	93	11
O_2	6		
Ar	20	62	7
CO_2	9	62	11
H_2O	<30	145	11

saturation is conveniently given by the ratio of the satellite $Q_1'(4)$ transition to the main $Q_1(4)$ branch in excitation scans; when the laser power is increased so that a nonlinear response sets in, their ratio increases beyond the line strength ratio of 0.15.

The results are the collision free measurements under nearly linear excitation conditions is as follows: for the parallel orientation, at low intensities (10−20 μJ/pulse) the Q/P ratio is approximately 2.7, while at higher intensities (1 mJ/pulse) the Q/P ratio is 1.7. We do not fully attain the collision free limit but are close to it, within the uncertainty in the Q/P ratio measurement. In the runs below, the early values of the degree of polarization are slightly less. We attribute this discrepancy with calculation to an imperfectly polarized laser beam, and perhaps some residual partial saturation, but we cannot quantitatively account via measurement.

Collisional Depolarization of $N' = 4$. A measurement of the Q/P ratio as a function of time following the excitation laser pulse, in the presence of a collider, yields the rate of collisional depolarization. Figure 3 shows the Q/P ratio measured for parallel polarization, as a function of time at a pressure of 1.6 Torr of He. These data approach the depolarized ratio value of 1.4 at long time. (Helium is a poor quencher of OH, and therefore, the removal mechanism is radiative, with a lifetime of 700 ns.) The fact that the polarization at short time is not the collision-free value does not affect the rate determination. Cross sections are obtained by dividing the measured rate coefficient by the average thermal velocity. From the data in Figure 3, we estimate a collisional depolarization cross section for He, for the $F_1(4)$ level, of 3 Å^2. This can be compared with a total RET cross section[8] for the nearby $F_2(4)$ level of about 4 Å^2 for He.

Collisional depolarization cross sections for the $F_1(4)$ level were also measured for several other colliders. N_2, O_2, Ar, CO_2, and H_2O are all important colliders for applications of LIF to atmospheric and combustion monitoring. We measured the depolarization cross sections listed in Table 1, using the same Q/P ratio as a function of time that was illustrated for He. It is interesting for both fundamental studies and applications to compared with the cross sections for rotational energy tranfer out of the pumped level. These are also given in Table 1. It is seen that the collisional depolarization cross sections are smaller than the total rotational energy transfer.

Inelastic depolarization may be measured from the Q/P ratios for the other levels populated by rotational energy transfer. The data in Figure 4 show spectra obtained in helium by pumping $Q_1(4)$. Note the extensive rotational energy transfer at long times and the Q/P ratios for the various levels. Rotational energy transfer into the $F_1(3)$ retains some polarization, while rotational energy transfer into the $F_1(2)$ and $F_1(1)$ levels appear to completely depolarize the fluorescence. This degree of transfer of polarization has bearing in the application of scaling laws for rotational energy transfer, but our signals were not strong enough to measure it quantitatively.

Collisional Depolarization from Other Levels. Elastic depolarization rates were also measured for $F_1(2)$ and $F_1(1)$ in helium (Figure 5). The cross sections are 6 and 9 Å^2 respectively. Classically this can be understood by considering a spinning top—as the top spins slower, a bump more easily perturbs the orientation of the top. Quantum mechanically, the lower J levels have fewer m_J values and we would expect that a collision of a molecule in a lower J level would result in a larger perturbation of the orientation of the molecule. Thus, the results for the lower levels are not surprising. We would therefore expect that the depolarization rates for higher J levels should be smaller than those measured for $F_1(4)$.

Applications

We can use our depolarization results to understand the previous results obtained in the burnt gases region of an atmospheric pressure methane/air flame. The relative rates for quenching, rotational energy transfer and depolarization can be compared (we will consider the $v' = 0$ case, where vibrational energy transfer is not involved). Quenching can be calculated from quenching cross sections estimated at 2000 K.[8] The result is 4×10^8 s^{-1} with approximately 82% of the quenching caused by water present at a mole fraction of 0.18. Similarly, rotational energy transfer can be estimated from room-temperature measurements of RET rate coefficients[9] as 1.8×10^9 s^{-1}. An upper limit for the depolarization rates can also be estimated from our rate coefficients for $F_1(4)$ as $<4.9 \times 10^8$ s^{-1}; about a third of this comes from water, for which we were only able to obtain an upper limit for the rate constant. For the higher N' levels present at flame temperatures, we would expect the depolarization rates to be even smaller. Thus, the depolarization rate is less than one-quarter of the other removal rates. We expect the fluorescence emission in the burnt gases region of a methane/air flame to be highly polarized, requiring that polarization be considered when designing a detection system for the fluorescence.

A model has been developed by Kohse-Höinghaus and coworkers to analyze fluorescence signals.[9] This model uses rate equations to describe the time-dependent populations, accounting for all relevant collisional and radiative processes; the model can be used to develop procedures using LIF to measure concentrations and temperatures. These depolarization results can now be incorporated into this model to study polarization effects in fluorescence determinations.

These results can also be applied to atmospheric monitoring experiments where OH concentrations are measured using LIF.[10] In this application, the OH is present at far smaller concentrations than in flames, on the order of 0.1 part per trillion in the troposphere. To reduce interference from laser photolysis of ozone, most of the atmospheric measurements are made at low pressure, approximately 4 Torr, where the OH fluorescence signal has a lifetime of several hundreds of nanoseconds. Electronic gating is used to discriminate against laser scatter and fluorescence from aerosols, SO_2, and CH_2O which are present in the first 30−50 ns. A typical gate is 400 ns wide with a delay of 250 ns at the 4 Torr pressure, encompassing a large fraction of the LIF signal from OH. During this measurement time, the rotational population distribution shifts due to collisions, leading to changes in quenching rate, and the polarization of the fluorescence will also evolve. The rate equation model can be used to simulate the fluorescence quantum yield for different ambient atmospheric conditions in these experiments as well.

Acknowledgment. This work was supported by the National Science Foundation Division of Atmospheric Chemistry.

References and Notes

(1) Doherty, P. M.; Crosley, D. R. *Appl. Opt.* **1984**, *23*, 713.
(2) Altkorn, R.; Zare, R. N. *Annu. Rev. Phys. Chem.* **1984**, *35*, 265.
(3) Smyth, K. C.; Crosley, D. R. In *Applied Combustion Diagnostics*; Kohse-Höinghaus, K., Jeffries, J. B., Eds.; Taylor and Francis: New York, 2002; Chapter 2, p 9.
(4) Crosley, D. R. *J. Atmos. Sci.* **1995**, *52*, 3299.
(5) Drier, T.; Ewart, P. In *Applied Combustion Diagnostics*; Kohse-Höinghaus, K., Jeffries, J. B., Eds.; Taylor and Francis: New York, 2002; Chapter 3, p 69.
(6) Jörg, A.; Degli Esposti, A.; Werner, H.-J. *J. Chem. Phys.* **1990**, *93*, 8757.
(7) Degli Esposti, A.; Werner, H.-J. *J. Chem. Phys.* **1990**, *93*, 3351.
(8) Tamura, M.; Berg, P.; Luque, J.; Jeffries, J. B.; Smith, G. P.; Crosley, D. R. *Combust. Flame* **1998**, *114*, 502.
(9) Keinle, R.; Lee, M. P.; Kohse-Höinghaus, K. *Appl. Phys. B: Laser Opt.* **1996**, *62*, 583.
(10) Crosley, D. R. In *Current Problems and Progress in Atmospheric Chemistry*; Barker, J. R., Ed.; World Scientific Publishing: Singapore, 1995; p 256.
(11) Jörg, A.; Meier, U.; Kienle, R.; Kohse-Höinghaus, K. *Appl. Phys. B: Laser Opt.* **1992**, *55*, 305.